

## Preparation and characterization of L-phenylalanine-derivatized $\beta$ -cyclodextrin-bonded silica and its application on chiral separation of alanine acid racemates

Kaichen He, Fengxian Qiu<sup>†</sup>, Jiao Qin, Jie Yan, and Dongya Yang

School of Chemistry and Chemical Engineering, Jiangsu University, Zhenjiang 212013, P. R. China  
(Received 1 July 2013 • accepted 20 August 2013)

**Abstract**—A chiral adsorption material, L-phenylalanine-derivatized  $\beta$ -cyclodextrin-bonded silica (L-Phe-CD/SiO<sub>2</sub>), was prepared and characterized by Fourier transform infrared (FT-IR), elemental analysis, field emission scanning electron microscope (FESEM), differential scanning calorimetry (DSC) and thermogravimetric analysis (TG) measurements. Langmuir and Freundlich isotherm models were employed to simulate the equilibrium data. The results showed that the equilibrium data were well represented by Langmuir isotherm model. Experimental data were analyzed using pseudo-first order and pseudo-second order kinetic models and the obtained results indicated that kinetics followed a pseudo-second order equation. The static adsorption experiments indicated that L-Phe-CD/SiO<sub>2</sub> had significantly higher adsorption capacity for L-alanine (L-Ala) compared with D-alanine (D-Ala); and the selectivity coefficient is 2.53. The result shows that the prepared L-Phe-CD/SiO<sub>2</sub> could be applied to chiral separation of the racemic alanine acid solution.

Key words:  $\beta$ -Cyclodextrin, Chiral Separation, Adsorption Isotherm, Kinetic Model, Thermodynamics Parameters

### INTRODUCTION

Chiral amino acids are one of the most important biomolecules due to the relevance in nature and their chemical richness [1]. In nature amino acids occur in L-forms and they play an important role in the food and pharmaceutical fields, while D-forms were discovered in species of lower animals, mammalian organs and blood. Some D-form amino acids were also detected in various vegetables and fruits. A small amount of D-alanine was found in freshly pressed plant juices [2]. It has been recognized that enantiomers have identical physical and chemical properties except for optical rotation. Because of these similarities, chiral discrimination of enantiomers is very challenging.

Cyclodextrins (CDs) are natural macrocyclic polymers of glucose that contain from six to eight D-(+)-glucopyranose units linked by  $\alpha$ -1,4-glucose bonds. The interior of the cavity, which contains two rings of C-H groups with a ring of glycosidic oxygen in between, is relatively hydrophobic, while the external faces with hydroxyl groups are hydrophilic [3-5]. Due to this special structure, they can selectively include some guest molecules into their hydrophobic cavities to form inclusion compounds with different stabilities. In specific cases involving CDs, the formation of an inclusion compound seems to be a fundamental part of the chiral recognition and separation process [6].

L-Phenylalanine is an amino acid containing the benzyl side group [7]. It is expected that addition of L-phenylalanine to CD could introduce additional interactions including hydrogen-bonding, complexation, ion-exchange, and hydrophobic and  $\pi$ - $\pi$  interactions, which leads to a change in the separation selectivity of the CD stationary phases. A wide variety of modified CD-bonded phases for enantioseparation were synthesized by Armstrong and his co-workers,

which not only in reversed-phase systems but also in normal phase systems [8]. An amino-modified CD-bonded phase was prepared by Hattori and co-workers [9], which suggested the occurrence of “host-guest chromatography” with multipoint recognition. Feng et al. [6] reported the synthesis of L-tyrosine-derivatized  $\beta$ -CD-bonded silica stationary; and the chromatographic performance in the reversed phase mode was evaluated by using positional isomers, organic acids and dansyl amino acids as solutes. Yu and co-workers [10] reported modified cyclodextrins and their inclusion complexation thermodynamics with L-tryptophan and some naphthalene derivatives. They also reported the molecular recognition behaviors of inclusion complex toward bile salts [11], showing the enhanced binding abilities. Recently, Wang et al. synthesized and analytically characterized methoxyethylamine monosubstituted  $\beta$ -cyclodextrin, mono-6<sup>A</sup>-(2-methoxyethyl-1-ammonium)-6<sup>A</sup>- $\beta$ -cyclodextrin chloride, appearing to outstanding enantioselectivities toward ampholytic and acidic racemates in capillary electrophoresis [12]. Paik and his co-workers synthesized a series of novel chiral mesoporous silica (CMS) spheres and chiral-mesoporous-polyppyrole (CMPPy) nanoparticles, which with high surface areas can be used for chiral separation of enantiomers and obtained quite good results [13-16]. These above-mentioned chiral separations techniques have proven their value, offering good selectivity and low limits of quantification; however, they may also require lengthy and expensive method development and prolonged analysis times. Therefore, much attention has been paid recently to the development of selecting high efficiency, low cost and wide applicability method of separation chiral enantiomers.

The aim of this work was to prepare a novel chiral adsorption material, L-phenylalanine-derivatized  $\beta$ -CD-bonded silica (L-Phe-CD/SiO<sub>2</sub>), and develop adsorption behavior of L-Phe-CD/SiO<sub>2</sub> in order to understand the host-guest interaction in-depth. The experimental data obtained from the equilibrium studies were fitted to Langmuir and Freundlich adsorption models. Kinetic studies were also carried out to determine the characters of adsorption process [17,18].

<sup>†</sup>To whom correspondence should be addressed.  
E-mail: fxqiuchem@163.com

## EXPERIMENTAL

## 1. Materials

$\beta$ -Cyclodextrin ( $\beta$ -CD) was obtained from Sinopharm Chemical Reagent Co. Ltd., (Shanghai, China) and purified by recrystallization from water and then dried at 100 °C under vacuum for 24 h. L-alanine (L-Ala), D-alanine (D-Ala), L-phenylalanine and pyridine (80%) were purchased from Sinopharm Chemical Reagent Co. Ltd., (Shanghai, China). *p*-Toluenesulfonyl chloride was recrystallized. DMF and pyridine were dried and redistilled before use. 3-Glycidoxypropyltrimethoxysilane was supplied by the Chemical Reagent Corporation (Shanghai, China). A spherical silica gel (5–7  $\mu$ m, approximately surface area of 210 m<sup>2</sup> g<sup>-1</sup>) was purchased from Qingdao Sea Chemical Plant (Qingdao, China). Other chemicals and reagents were of analytical grade and used as received.

## 2. Activation of Silica Gel

Silica gel (10 g) was immersed in conc. HCl-H<sub>2</sub>O (1 : 3, v/v; 200 mL) for 24 h and refluxed at 120 °C under stirring for 10 h. After that, the activated silica gel was filtered and washed with doubly distilled water to neutral. Finally, the product was dried at 150 °C for 10 h, and kept in a desiccator before use. Activated silica gel was obtained.

3. Preparation of CD/SiO<sub>2</sub> (I)

To a solution of  $\beta$ -CD (6.0 g) dissolved in anhydrous DMF (100 mL), NaH (0.3 g) was added. The mixture was stirred at room temperature until no hydrogen was emitted, and the excessive NaH removed by filtration. Thereafter, 2.0 mL of 3-glycidoxypropyltriethoxysilane as the role of silicone coupling agent was added to the filtrate and participated in the coupling reaction accompanied with ring-opening process, which was allowed to react at 90 °C for 5 h under an inert atmosphere of nitrogen gas. After cooling to room temperature, activated silica gel (5.0 g) was added and the system was kept stirring at 110–120 °C for 24 h. The product (CD/SiO<sub>2</sub>)

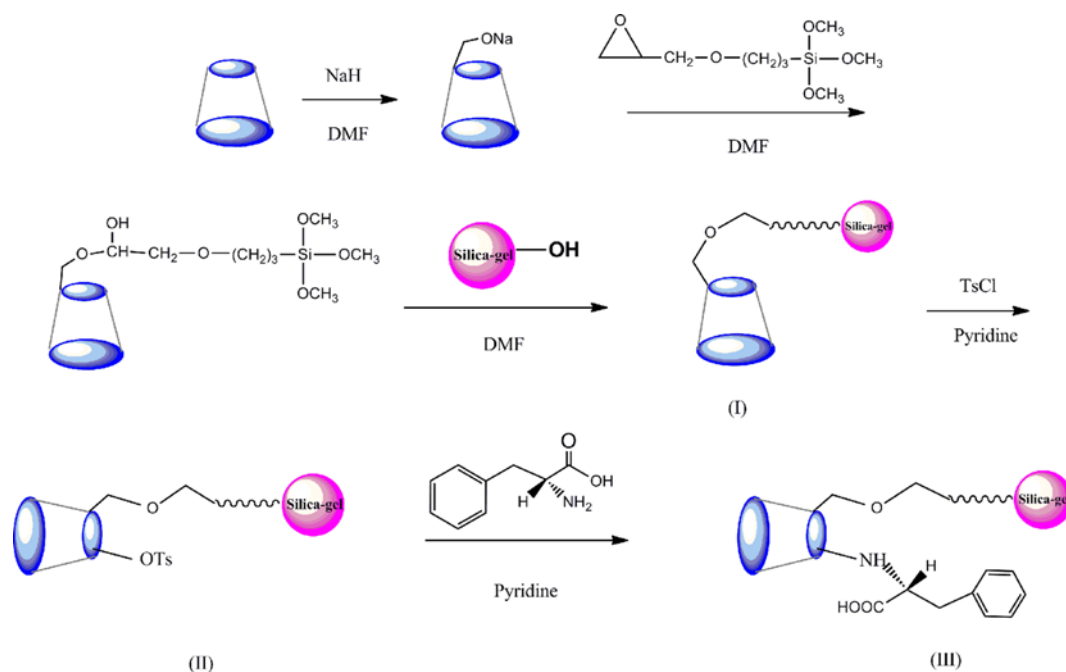
was filtered, stirred and washed with DMF, doubly distilled water, methanol and acetone for 30 min at 25 °C in sequence. Subsequently, the CD/SiO<sub>2</sub> (I) was dried at 120 °C for 3 h, cooled and kept in a desiccator before use.

4. Preparation of L-Phe-CD/SiO<sub>2</sub> (III)

To a solution of *p*-toluenesulfonyl chloride (2.0 g) dissolved in dry pyridine (50 mL), CD/SiO<sub>2</sub> (2.0 g) was added. After stirring at room temperature for 24 h and at 0–5 °C for 18 h, the product tosylated- $\beta$ -CD-bonded silica gel (TsCD/SiO<sub>2</sub>) (compound II) was filtered and washed with pyridine, diethyl ether, methanol and diethyl ether at 25 °C for 30 min in sequence [19]. After drying in vacuo over P<sub>2</sub>O<sub>5</sub> for 24 h, the TsCD/SiO<sub>2</sub> (2.0 g) was suspended in dry pyridine (50 mL) containing L-phenylalanine (2.0 g). The mixture was allowed to react at 80 °C for 48 h with stirring under nitrogen. After cooling to room temperature, the reaction mixture was filtered. The product L-Phe-CD/SiO<sub>2</sub> was washed with diethyl ether, ethanol, diluted hydrochloric acid, distilled water and acetone at 25 °C for 30 min in sequence. Subsequently, the material was dried at 120 °C for 4 h and kept in a desiccator before being used [6]. The synthetic route of the L-phenylalanine-derivatized  $\beta$ -cyclodextrin-bonded silica (L-Phe-CD/SiO<sub>2</sub>, III) is shown in Scheme 1.

## 5. Characterization

FT-IR spectra of samples were obtained between 4,000 and 400 cm<sup>-1</sup> on a KBr palette with an FT-IR spectrometer (AVATAR 360, Nicolet, USA). UV spectra were recorded on a Shimadzu UV-2450 spectrophotometer (Kyoto, Japan) equipped with a TCC-240A thermoelectrically temperature controlled cell holder between 183 and 400 nm in a quartz cell of 1 cm path length. Differential scanning calorimetry (DSC) and thermogravimetric analysis (TG) were recorded on a Netzsch (Germany) STA 449C instrument. The programmed heating range was from room temperature to 800 °C at a heating rate of 10 °C min<sup>-1</sup> under a nitrogen atmosphere. The measurement was taken with 7.545 mg sample. Optical rotation was performed



Scheme 1. The synthetic route of the L-phenylalanine-derivatized  $\beta$ -cyclodextrin-bonded silica (L-Phe-CD/SiO<sub>2</sub>).

with a WXG-4 visual spin spectrometer (Shanghai Optical Instruments Factory, China). The surface of the sample was investigated with a 15-kV accelerating voltage with a field emission scanning electron microscope (FESEM) (S-4800, Hitachi Corp., Tokyo, Japan). Vario EL elemental analyzer (Elementar, Hanau, Germany) was employed to investigate the surface elemental composition of the particles.

### 6. Adsorption Experiment

To an aliquot solution of the L-Ala or D-Ala dissolved in water (50 mL), chiral L-Phe-CD/SiO<sub>2</sub> (0.02 g) was added to a conical flask. The resultant solution was shaken and equilibrated at room temperature in a water thermostat bath. After stirring for 12 h, the absorbance of the remaining solution in supernatant was measured by UV-2450 spectrophotometer at 190 nm after centrifugation. The concentration was determined through a calibration curve for the known L-Ala or D-Ala concentration in the individual aqueous solution. The adsorption capacity of L-Phe-CD/SiO<sub>2</sub> was calculated according to the following Eq. (1) [20]:

$$Q_e = \frac{(C_0 - C_e)V}{M} \quad (1)$$

where  $Q_e$  is the equilibrium adsorption capacity of the L-Phe-CD/SiO<sub>2</sub> (mg g<sup>-1</sup>);  $V$  is the solution volume (mL);  $C_0$  is the initial concentration of alanine acid (L-Ala or D-Ala) (mg L<sup>-1</sup>);  $C_e$  is the equilibrium concentration of alanine acid (L-Ala or D-Ala) (mg L<sup>-1</sup>); and  $M$  is the mass of the L-Phe-CD/SiO<sub>2</sub> (g).

### 7. Selectivity Experiment

To a 50 mL racemic solution (0.3 g L<sup>-1</sup>, optical rotation is zero, molar ratio of L-Ala and D-Ala was 1 : 1), L-Phe-CD/SiO<sub>2</sub> (0.02 g) was added to a conical flask. The resultant solution was transferred to a 50 mL tube and was shaken and equilibrated at room temperature in a water thermostat bath. A specified time later, the absorbance of remaining solution in supernatant was measured by spectrophotometer at 190 nm after centrifugation. Optical rotation and specific optical rotation of remaining solution in supernatant were measured by polarimeter (Specific Rotation  $[\alpha]$  is -1.32°). The concentration was obtained through a calibration curve for the known concentration in the individual aqueous solution.

In this experiment, the direction of the optical rotation was the same as D-Ala. The distribution coefficient for each substance was calculated according to the following Eq. (2) to (4) [21]:

$$C_{D,e} = \left( \frac{[\alpha]}{[\alpha]_{D,S}} + \frac{1 - \frac{[\alpha]}{[\alpha]_{D,S}}}{2} \right) \times 100\% \times C_{t,e} \quad (2)$$

$$C_{L,e} = C_{t,e} - C_{D,e} \quad (3)$$

where  $C_{D,e}$  and  $C_{L,e}$  are concentrations of D-Ala and L-Ala in remaining solution in supernatant (mg L<sup>-1</sup>), respectively;  $[\alpha]$  is the

specific optical rotation of remaining solution in supernatant;  $[\alpha]_{D,S}$  is standard specific optical rotation of D-Ala;  $C_{t,e}$  is the total equilibrium concentration of the supernatant (mg L<sup>-1</sup>).

$$K_d = \frac{Q_e}{C_e} \quad (4)$$

where  $K_d$  represents the distribution coefficient (mL g<sup>-1</sup>);  $Q_e$  is the equilibrium binding amount (mg g<sup>-1</sup>); and  $C_e$  is the equilibrium concentration (mg mL<sup>-1</sup>).

The selectivity coefficient ( $K$ ) of L-Phe-CD/SiO<sub>2</sub> for L-Ala relative to D-Ala allows an estimation of selectivity, which is obtained according to Eq. (5):

$$K = \frac{K_{d(L-Ala)}}{K_{d(D-Ala)}} \quad (5)$$

## RESULTS AND DISCUSSION

### 1. Characterization of Chiral L-Phe-CD/SiO<sub>2</sub>

Preparation of CD-bonded silica gel has been studied extensively [22-26]. In this study,  $\beta$ -CD/SiO<sub>2</sub> was prepared by a batch method in which the product would be purified only through washing with appropriate solvents [6]. The obtained CD/SiO<sub>2</sub> was the white powder. The L-Phe-CD/SiO<sub>2</sub> was synthesized by the reaction of L-phenylalanine with TsCD/SiO<sub>2</sub>; and the product was yellow. The typical carbon, hydrogen and nitrogen content of the CD/SiO<sub>2</sub> and L-Phe-CD/SiO<sub>2</sub>, which were measured by Vario EL elemental analyzer, is given in Table 1. The concentration of  $\beta$ -CD in the CD/SiO<sub>2</sub> was calculated as the carbon content, while the concentration of  $\beta$ -CD in the L-Phe-CD/SiO<sub>2</sub> was calculated as carbon and nitrogen content. And the concentration of L-phenylalanine was calculated as nitrogen content. The concentration of  $\beta$ -CD in the CD/SiO<sub>2</sub> and L-Phe-CD/SiO<sub>2</sub>, and the concentration of L-phenylalanine attached to  $\beta$ -CD on the L-Phe-CD/SiO<sub>2</sub> were estimated from the results of elemental analysis according to their structures depicted in Scheme 1, and were found, as shown in Table 1, to be 0.152 and 0.192 mmol g<sup>-1</sup>, respectively. The results suggest that L-phenylalanine molecules were successfully attached to CD/SiO<sub>2</sub> and approximately 1.26 L-phenylalanine molecules were attached to one CD/SiO<sub>2</sub>. The concentration of  $\beta$ -CD in L-Phe-CD/SiO<sub>2</sub> was less than that of the CD/SiO<sub>2</sub> because of the alkaline medium in the derivatization reaction process, which leads to some small part of  $\beta$ -CD molecules being taken off from the activated SiO<sub>2</sub>.

FT-IR spectra of activated SiO<sub>2</sub>, CD/SiO<sub>2</sub> and L-Phe-CD/SiO<sub>2</sub> are shown in Fig. 1. The characteristic absorption peak corresponding to the stretching vibrations of free and hydrogen-bonded O-H groups are observed at 3,450 cm<sup>-1</sup>. The band around 1,058 cm<sup>-1</sup> corresponds to the stretching vibrations of Si-O-Si and Si-O-H groups. The absorption bands around 798 and 485 cm<sup>-1</sup> are attributed to the stretching vibrations of Si-O. Compared with spectrum of SiO<sub>2</sub>, the

**Table 1. Elemental analysis results of CD/SiO<sub>2</sub> and L-Phe-CD/SiO<sub>2</sub>**

Materials	C (%)	N (%)	H (%)	$\beta$ -CD concentration (mmol g <sup>-1</sup> )	L-phenylalanine concentration (mmol g <sup>-1</sup> )
CD/SiO <sub>2</sub>	7.11	0.0	1.31	0.168	0.0
L-Phe-CD/SiO <sub>2</sub>	8.06	0.27	1.47	0.152	0.192

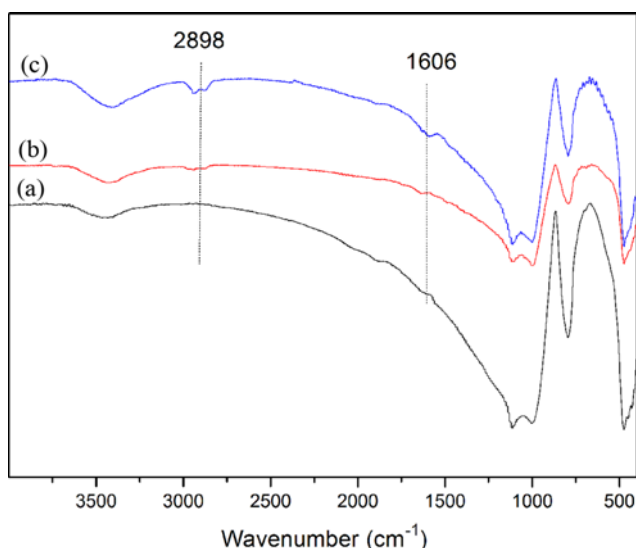


Fig. 1. FT-IR spectra of activated  $\text{SiO}_2$  (a),  $\text{CD/SiO}_2$  (b) and  $\text{L-Phe-CD/SiO}_2$  (c).

spectrum of  $\text{CD/SiO}_2$  displays new absorption peaks at 2,898 and 1,606  $\text{cm}^{-1}$ , which are attributed to the stretching vibration absorptions of saturated C-H band and carbonyl C=O in ester groups, respectively. These results indicate that  $\beta$ -CD had been grafted successfully onto the surface of  $\text{SiO}_2$ . Compared with  $\text{CD/SiO}_2$ , the spectrum of  $\text{L-Phe-CD/SiO}_2$  shows that the stretching vibration absorptions of saturated C-H band and carbonyl C=O in ester groups are strengthened distinctly. The infrared data proved that the  $\text{L-Phe-CD/SiO}_2$  had been obtained.

## 2. FESEM Analysis

In most cases, surface morphology of material is of great importance for many technical applications requiring well-defined surfaces or interfaces. The FESEM morphologies of activated  $\text{SiO}_2$  and  $\text{L-Phe-CD/SiO}_2$  are shown in Fig. 2. The spherical and regular structures of activated  $\text{SiO}_2$  are observed in Fig. 2(a). Compared with activated  $\text{SiO}_2$ , the shape of the cavities of  $\beta$ -CD, the structures of L-phenylalanine and spherical activated  $\text{SiO}_2$  are all observed from Fig. 2(b), which are due to the derivatization reaction process in the dry pyridine. The result suggested that  $\beta$ -CD was successfully introduced onto the surface of the activated  $\text{SiO}_2$ , which is benefi-

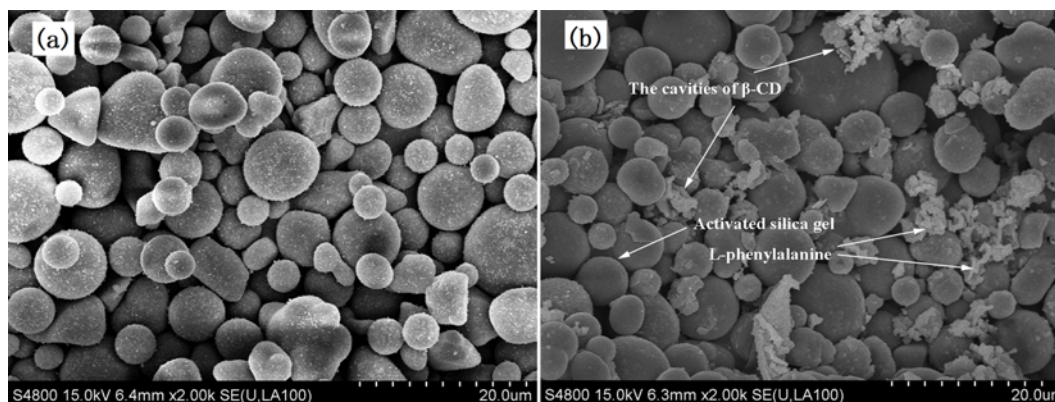


Fig. 2. SEM images of activated  $\text{SiO}_2$  (a) and  $\text{L-Phe-CD/SiO}_2$  (b).

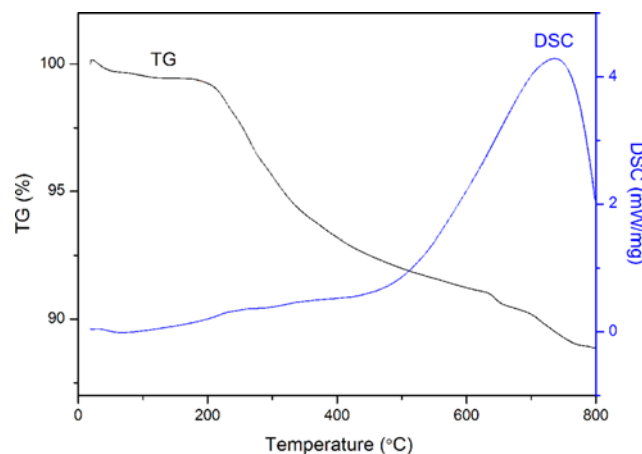


Fig. 3. DSC and TG curves of  $\text{L-Phe-CD/SiO}_2$ .

cial for the adsorption of Ala molecules.

## 3. Thermal Property of Chiral $\text{L-Phe-CD/SiO}_2$

To examine the thermal stability of  $\text{L-Phe-CD/SiO}_2$ , differential scanning calorimetry (DSC) and thermogravimetric analysis (TG) were performed; and the results are shown in Fig. 3. As can be seen, there are two steps (at  $T < 200$  °C and 200–800 °C, respectively) in TG curves of the  $\text{L-Phe-CD/SiO}_2$ . The first weight loss of 1.8% might be ascribed to the loss of the physisorbed water. Because of the low rate of the weight loss, there is no obvious endothermic peak from the DSC curve during this temperature range. Therefore, the structure of  $\text{L-Phe-CD/SiO}_2$  is stable and can be used for the chiral separation at  $T < 200$  °C. The other weight loss of 10.2% at 200–800 °C might be attributed to the decompositions of organic moieties, which correspond to the endothermic peaks at 737 °C at the DSC curves. And rest part of weight belongs to the remaining organic moieties and residual activated  $\text{SiO}_2$ .

## 4. Effects of Adsorption Conditions on the Recognition Selectivity of $\text{L-Phe-CD/SiO}_2$

The effect of the temperature on the adsorption efficiency of L-Ala solution onto the  $\text{L-Phe-CD/SiO}_2$  is shown in Fig. 4. Initially, the L-Ala adsorption efficiency increases with the increase of temperature due to the force between the adsorbent and L-Ala. However, as the temperature further increases, the adsorption efficiency decreases. This is mainly due to the collapse of intermolecular attrac-

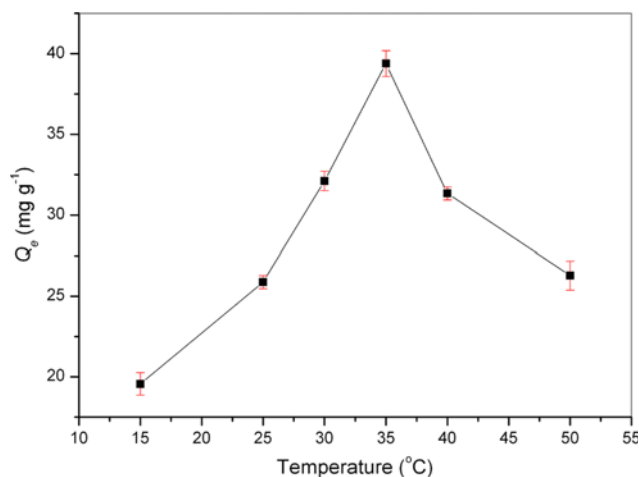


Fig. 4. The effect of the temperature on the adsorption efficiency of L-Ala solution onto the L-Phe-CD/SiO<sub>2</sub>.

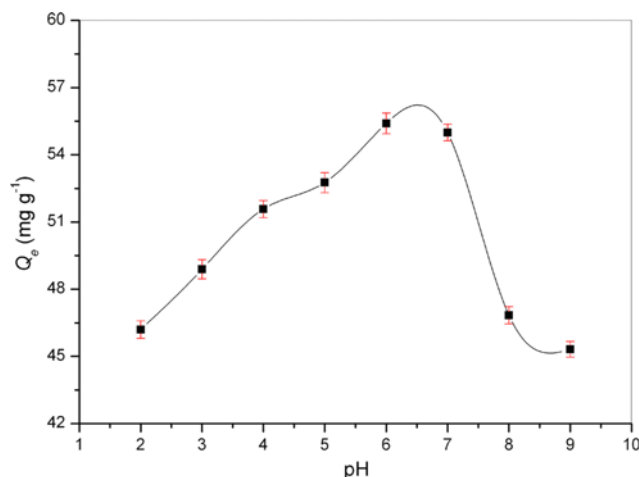


Fig. 6. The effect of pH on L-Ala adsorption was studied within the range of 2-9.

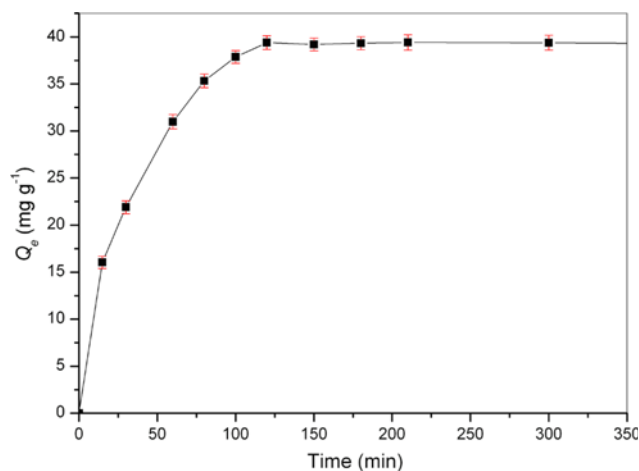


Fig. 5. The effect of the contact time on the adsorption efficiency of L-Ala solution at 35 °C.

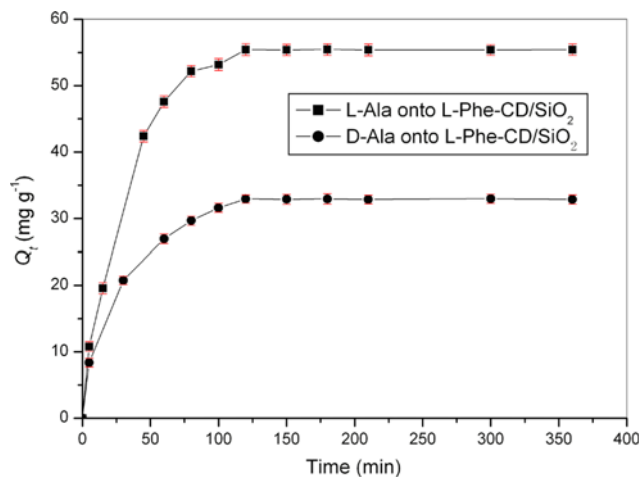


Fig. 7. The adsorption kinetic curves of L-Ala and D-Ala onto L-Phe-CD/SiO<sub>2</sub>.

tion. When the temperature was 35 °C, the highest L-Ala adsorption efficiency was obtained. Therefore, the temperature of 35 °C was chosen for the further study of L-Ala adsorption.

The effect of the contact time on the adsorption efficiency of L-Ala solution at 35 °C is shown in Fig. 5. At the initial adsorption stage, the adsorption efficiency increases very quickly with time prolonging, then it increases slowly. And it is nearly unchangeable when time is more than 2.0 h. The rapid adsorb might be due to the adsorption sites being void and the fast interactions between L-Ala and the surface of the material, and then reaching adsorption equilibrium. The experimental results indicated that 2.0 h was sufficient to reach adsorption equilibrium for the L-Ala. Therefore, 2.0 h was selected as the optimum contact time for the further study.

Another important factor in adsorption studies is the effect of pH of the solution. It can influence the protonation of the functional groups on the adsorbents as well as the solution chemistry (for example, hydrolysis, complexation, and redox reaction). The effect of pH on L-Ala adsorption was studied within the pH range of 2-9, and the results are shown in Fig. 6. It is evident that the adsorption efficiency increases with the increase of pH ranging from 2.0-6.0.

Then, the adsorption is maintained at about the same level with the pH of 6.0-7.0. At pH > 7.0, the adsorption efficiency decreases with the increase of pH value. The main reason for these results can be ascribed to following. The L-Phe-CD/SiO<sub>2</sub> has permanent positive charges on its surface, at lower pH ranging from 2.0-6.0; L-Ala molecules also have positive charges on their surface. With the pH reaching 6.0, the charges of L-Ala molecules on the surface have become negative. Therefore, the adsorption efficiency has increased. Continuing to increase the pH > 7, the competition is increased with the increase of OH<sup>-</sup>, which results in low adsorption efficiency.

In conclusion, the adsorption conditions of L-Ala are as follows: time of 2.0 h, temperature of 35 °C, and pH between 6.0 and 7.0.

### 5. Adsorption Kinetics

The adsorption kinetic curves of L-Ala and D-Ala onto L-Phe-CD/SiO<sub>2</sub> material at the optimum condition according to Eq. (1) are shown in Fig. 7. The adsorption amounts of L-Ala and D-Ala on L-Phe-CD/SiO<sub>2</sub> increased quickly with the time during the first 80 min and then increased slowly with the time and about 120 min later; the adsorption process reaches equilibrium. Moreover, the adsorption amounts of L-Ala on L-Phe-CD/SiO<sub>2</sub> are higher than that

of D-Ala on L-Phe-CD/SiO<sub>2</sub> after the adsorption equilibrium. It is reasonable to assume that some chiral recognition sites exist on the surface of L-Phe-CD/SiO<sub>2</sub>, so L-Ala is easy to combine with adsorption material and bind with the chiral recognition sites. However, the chiral recognition sites do not fit for D-Ala, which results in lower adsorption amounts of D-Ala on L-Phe-CD/SiO<sub>2</sub> after the adsorption equilibrium.

It is important to be able to predict the rate at which a solute is removed from ethanol solutions in order to design an adsorption treatment plant. To evaluate adsorption kinetics, two common models were applied to the experimental data obtained at adsorption processes.

#### 5-1. Pseudo-first-order Kinetic Equation

The pseudo-first order [27] kinetic model is expressed as the following Eq. (6):

$$\frac{dQ_e}{dt} = k_1(Q_e - Q_t) \quad (6)$$

where  $Q_e$  and  $Q_t$  are the amounts of solute adsorbed per unit amount of L-Phe-CD/SiO<sub>2</sub> at equilibrium and any time,  $t$ , respectively (mg

g<sup>-1</sup>) and  $k_1$  is the pseudo-first-order rate constant (min<sup>-1</sup>).

Integrating Eq. (6) employing the boundary conditions that at  $t=0$ ,  $Q_t=0$ ; and that at  $t=t$ ,  $Q_t=Q_t$ , the linear form of the equation becomes:

$$\ln(Q_e - Q_t) = \ln Q_e - k_1 t \quad (7)$$

The adsorption rate constant,  $k_1$  (min<sup>-1</sup>), can be obtained from the slope of the linear plot of  $\ln(Q_e - Q_t)$  versus  $t$ .

#### 5-2. Pseudo-second-order Equation

The pseudo-second order [28] kinetic model is expressed as the following Eq. (8):

$$\frac{dQ_e}{dt} = k_2(Q_e - Q_t)^2 \quad (8)$$

where  $k_2$  is the pseudo-second-order rate constant (g mmg<sup>-1</sup> min<sup>-1</sup>). On integration, employing the conditions that at  $t=0$ ,  $Q_t=0$ ; and that at  $t=t$ ,  $Q_t=Q_t$ , this equation can be re-arranged to give the linear form:

$$\frac{t}{Q_t} = \frac{1}{k_2 Q_e^2} + \frac{t}{Q_e} \quad (9)$$

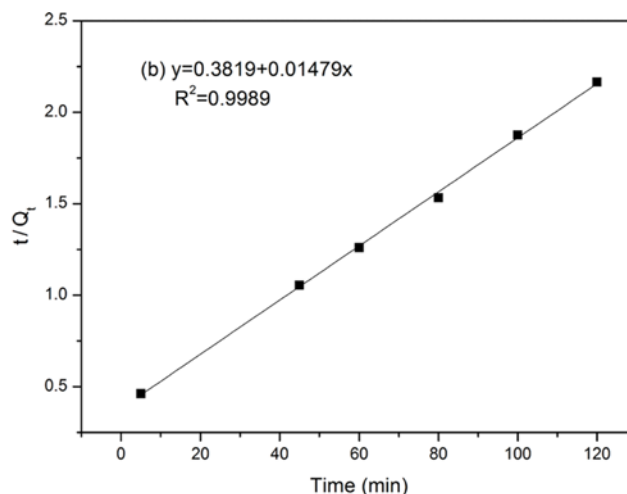
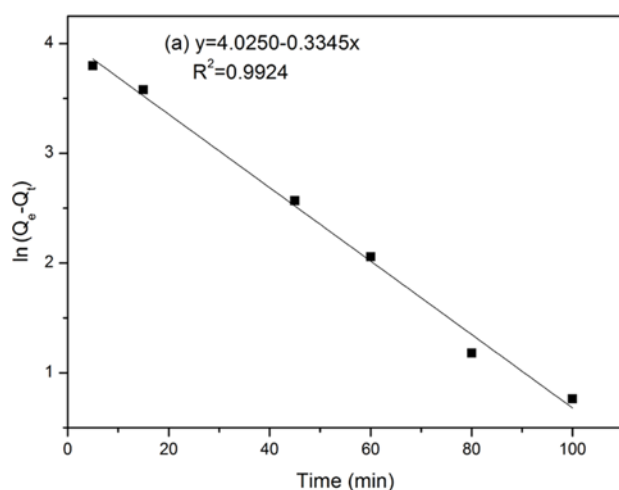


Fig. 8. The kinetic models of the effect of temperature on adsorption of L-Ala onto L-Phe-CD/SiO<sub>2</sub>.

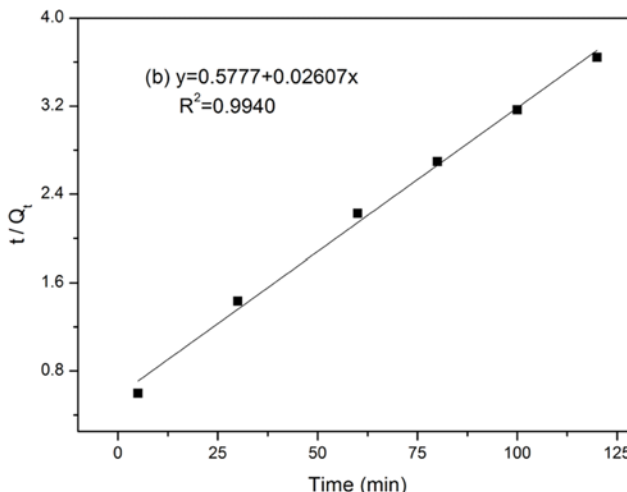
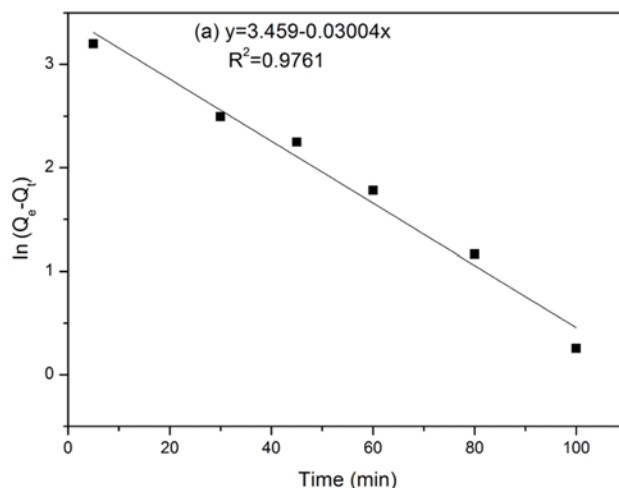


Fig. 9. The kinetic models of the effect of temperature on adsorption of D-Ala onto L-Phe-CD/SiO<sub>2</sub>.



**Table 2. The fitting parameters for the adsorption of L/D-Ala onto L-Phe-CD/SiO<sub>2</sub>**

Materials	Pseudo-first order			Pseudo-second-order		
	k <sub>1</sub> (min <sup>-1</sup> )	Q <sub>e</sub> (mg g <sup>-1</sup> )	R <sup>2</sup>	k <sub>2</sub> (g mg min <sup>-1</sup> )	Q <sub>e</sub> (mg g <sup>-1</sup> )	R <sup>2</sup>
L-Ala	0.3345	55.98	0.9924	5.728 × 10 <sup>-4</sup>	67.61	0.9989
D-Ala	0.03004	31.78	0.9761	1.1764 × 10 <sup>-3</sup>	38.36	0.9940

**Table 3. Adsorption isotherms parameters for L-Ala and D-Ala onto L-Phe-CD/SiO<sub>2</sub>**

Adsorption isotherms	T (K)	Langmuir			Freundlich			
		Q <sub>m</sub> (mg g <sup>-1</sup> )	b (L mg <sup>-1</sup> )	R <sup>2</sup>	R <sub>L</sub>	K <sub>f</sub>	1/n	R <sup>2</sup>
L-Ala	298	59.26	0.06292	0.9979	0.056-0.78	14.30	0.261	0.8906
	303	64.22	0.07768	0.9955	0.044-0.77	17.09	0.247	0.9004
	308	77.49	0.1554	0.9929	0.023-0.75	27.19	0.204	0.8563
	313	59.72	0.06835	0.9953	0.054-0.79	15.03	0.255	0.9098
	323	53.28	0.05438	0.9969	0.062-0.78	11.91	0.276	0.9035
D-Ala	298	26.64	0.03497	0.9984	0.011-0.30	4.686	0.307	0.9128
	303	33.10	0.04171	0.9986	0.012-0.33	6.414	0.292	0.9097
	308	41.22	0.04916	0.9953	0.13-0.37	8.769	0.279	0.9099
	313	30.74	0.03497	0.9940	0.11-0.30	5.148	0.316	0.9370
	323	23.96	0.02899	0.9960	0.10-0.27	3.500	0.335	0.9190

The plot of  $t/Q_t$  versus  $t$  gives a linear relationship, which allows the values of  $Q_e$  and  $k_2$  to be computed.

Fig. 8 and Fig. 9 show the kinetic models of the effect of temperature on adsorption of L-Ala and D-Ala onto L-Phe-CD/SiO<sub>2</sub>, respectively. The adsorption rate constants and linear regression values are summarized in Table 2. The adsorption model of L/D-Ala onto L-Phe-CD/SiO<sub>2</sub> follows pseudo-second-order kinetics because of the favorable fit between experimental and calculated values of  $Q_e$  ( $R^2$  of L-Ala and D-Ala are 0.9989 and 0.9940, respectively). Low  $R^2$  values of L-Phe-CD/SiO<sub>2</sub> for the first-order kinetic model suggest that L/D-Ala molecules are strongly held onto the binding sites of L-Phe-CD/SiO<sub>2</sub> by chemical bonds, involving valence forces through sharing or exchange of electrons between sorbent and adsorbate. And it is assumed that the adsorption process is a chemical process, which could be the rate-limiting step in the adsorption process.

## 6. Adsorption Isotherms

The adsorption of Ala enantiomers by L-Phe-CD/SiO<sub>2</sub> material was carried out at different initial concentrations. For a solid-liquid system, the equilibrium of sorption is one of important physico-chemical aspects in description of adsorption behavior. In this work, two important isotherm equations, namely Langmuir and Freundlich isotherms, were selected for the study of adsorption. The Langmuir isotherm assumes monolayer adsorption onto the surface containing a finite number of adsorption sites with no transmigration of the adsorbent in the plane of the surface [29]. This model, which is the most widely used two-parameter equation, generally can be expressed as the following Equation:

$$\frac{1}{Q_e} = \frac{1}{Q_m} + \frac{1}{bQ_m C_e} \quad (10)$$

where  $C_e$  is the equilibrium concentration of L-Ala or D-Ala in solution (mg L<sup>-1</sup>);  $Q_e$  is the amount of adsorbate adsorbed per unit mass of adsorbent (mg g<sup>-1</sup>);  $Q_m$  is the maximum adsorption capacity (mg

g<sup>-1</sup>); and  $b$  is the Langmuir adsorption constant which is related to the energy of adsorption (L mg<sup>-1</sup>). Plotting  $1/Q_e$  against  $1/C_e$  gives a straight line with slope and intercept equal to  $1/(bQ_m)$  and  $1/Q_m$ . All the isotherm parameters and the correlation coefficients,  $R^2$ , were calculated and summarized in Table 3.

Another important parameter,  $R_L$ , known as the separation factor, could be obtained from the relation:

$$R_L = \frac{1}{1 + bC_{ref}} \quad (11)$$

where  $C_{ref}$  is any equilibrium liquid phase concentration of the solute. It has been established that (i)  $0 < R_L < 1$  for favorable adsorption, (ii)  $R_L > 1$  for unfavorable adsorption, (iii)  $R_L = 1$  for linear adsorption, and (iv)  $R_L = 0$  for irreversible adsorption.

The Freundlich equation is a purely empirical relationship based on sorption onto a heterogeneous surface. This model, which has proved to be satisfactory for low concentrations, often represents an initial surface adsorption, followed by a condensation effect, resulting from extremely strong solute-solute interaction [30]. The linear form is commonly represented as:

$$\log Q_e = \log K_f + \frac{\log C_e}{n} \quad (12)$$

Although this equation was initially derived for adsorption from solution, it can also be used for adsorption from the gaseous or vapor phase, employing pressures rather than concentrations. In this equation,  $K_f$  and  $n$  are the Freundlich constants characteristic of the system, indicating the adsorption capacity and the adsorption intensity, respectively.  $K_f$  is defined as an adsorption or distribution coefficient representing the amount of solute adsorbed on an adsorbent for a unit equilibrium concentration, while  $n$  gives an indication of how favorable the adsorption process is. The slope of  $1/n$  ranging between 0 and 1 is a measure of adsorption intensity or surface het-

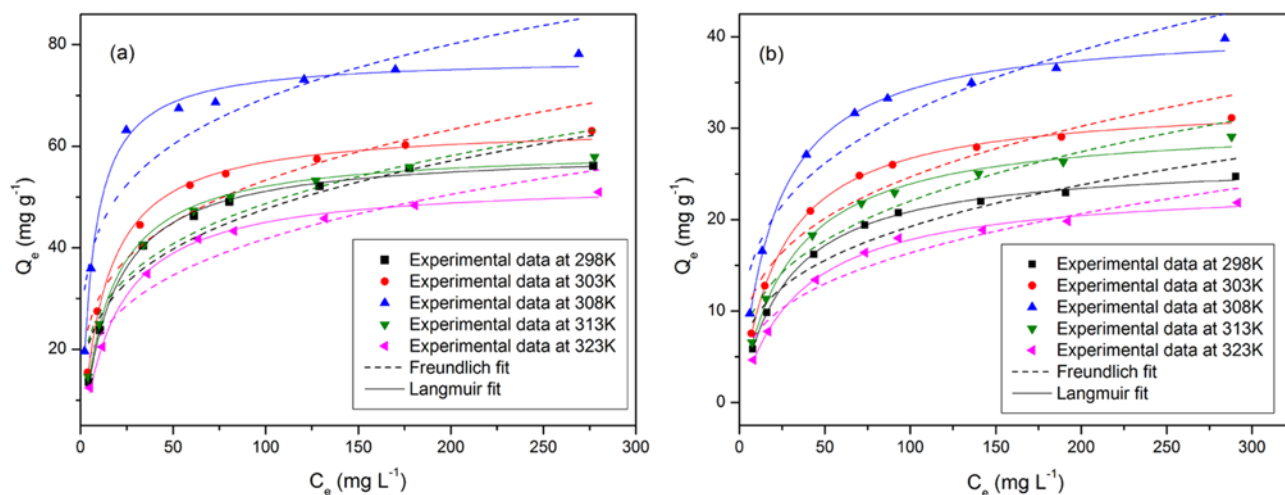


**Fig. 10.** The comparison of Langmuir and Freundlich isotherm models for L-Ala (a) and D-Ala (b) adsorption onto L-Phe-CD/SiO<sub>2</sub> using non-linear regression.

erogeneity, becoming more heterogeneous as its value gets closer to zero. A value for  $1/n$  below one indicates a normal Langmuir isotherm, while  $1/n$  above one is indicative of cooperative adsorption [31]. All the isotherm parameters and the correlation coefficients,  $R^2$ , were calculated and also summarized in Table 3.

The comparison of Langmuir and Freundlich isotherm models for L-Ala and D-Ala adsorption onto L-Phe-CD/SiO<sub>2</sub> using non-linear regression is shown in Fig. 10. As can be seen, when the equilibrium concentration increases, the equilibrium adsorption capacity ( $Q_e$ ) of L-Phe-CD/SiO<sub>2</sub> firstly increases sharply, then increases slightly, and finally reaches a maximum point. The Langmuir model with correlation coefficient represents a better fit of experimental data than the Freundlich isotherm, which indicates that the Langmuir model is more suitable to describe the L-Phe-CD/SiO<sub>2</sub> adsorption system. The values of the dimensionless constant  $R_L$  about L-Ala and D-Ala indicate that the adsorption is favorable and rather irreversible. Moreover, the maximum binding amounts ( $Q_{max}$ ) of L-Ala on L-Phe-CD/SiO<sub>2</sub> at 25 °C, 30 °C, 35 °C, 40 °C and 50 °C were 59.26 mg g<sup>-1</sup>, 64.22 mg g<sup>-1</sup>, 77.49 mg g<sup>-1</sup>, 59.72 mg g<sup>-1</sup> and 53.28 mg g<sup>-1</sup>, respectively; while  $Q_{max}$  of D-Ala on L-Phe-CD/SiO<sub>2</sub> at 25 °C, 30 °C, 35 °C, 40 °C and 50 °C were 26.64 mg g<sup>-1</sup>, 33.10 mg g<sup>-1</sup>, 41.22 mg g<sup>-1</sup>, 30.74 mg g<sup>-1</sup> and 23.96 mg g<sup>-1</sup>, respectively. These results suggest that the L-Phe-CD/SiO<sub>2</sub> has a higher adsorption ability of L-Ala than that of D-Ala. Furthermore, the  $Q_e$  of L-Phe-CD/SiO<sub>2</sub> firstly increases, then decreases with the temperature increase.

## 7. Thermodynamic Parameters

The thermodynamics for adsorption of Ala enantiomers on L-Phe-CD/SiO<sub>2</sub> is carried out with the temperature in the range of 298-

323 K. Thermodynamic parameters, that is, free energy ( $\Delta G^\circ$ ), enthalpy ( $\Delta H^\circ$ ), and entropy ( $\Delta S^\circ$ ), have been estimated to evaluate the feasibility and exothermic nature of the adsorption process. The Gibbs free energy change of the process is related to the equilibrium constant ( $K_p$ ) by the following equation [32].

$$\Delta G^\circ = -RT \ln K_p \quad (13)$$

$$K_p = \frac{Q_e}{C_e} \quad (14)$$

where  $K_p$  is distribution coefficient (L g<sup>-1</sup>).  $T$  is the absolute temperature in Kelvin, and  $R$  is the universal gas constant (8.314 J mol<sup>-1</sup> K<sup>-1</sup>).

According to thermodynamics, the Gibbs free energy change is also related to enthalpy change and entropy change at constant temperature by the following equation:

$$\ln K_p = \frac{-\Delta H^\circ}{RT} + \frac{\Delta S^\circ}{R} \quad (15)$$

According to Eq. (15), the values of  $\Delta H^\circ$  and  $\Delta S^\circ$  can be calculated from the slopes ( $\Delta H^\circ/R$ ) and intercepts ( $\Delta S^\circ/R$ ) of  $\ln K_p$  versus  $1/T$  plots. The calculated thermodynamic parameters are listed in Table 4. The negative value of all  $\Delta G^\circ$  indicated the feasibility of the process and spontaneous nature of Ala enantiomers adsorption onto L-Phe-CD/SiO<sub>2</sub> material. Moreover, the magnitude of  $\Delta G^\circ$  decreases from 298 K to 308 K, then increases from 308 K to 323 K with the increasing temperature, indicating that adsorption is favorable at 308 K. The positive value of  $\Delta H^\circ$  confirmed the endothermic

**Table 4.** Thermodynamic parameters for the adsorption of L-Ala and D-Ala on L-Phe-CD/SiO<sub>2</sub>

Adsorb material	L-Ala (298-308 K)			L-Ala (308-323 K)			D-Ala (298-308 K)			D-Ala (308-323 K)		
	298	303	308	308	313	323	298	303	308	308	313	323
$T$ (K)	298	303	308	308	313	323	298	303	308	308	313	323
$K_p$ (L g <sup>-1</sup> )	3.54	4.99	12.03	12.03	4.08	2.90	0.92	1.38	2.03	2.03	1.08	0.69
$\Delta G^\circ$ (KJ mol <sup>-1</sup> )	-3.13	-4.05	-6.37	-6.37	-3.66	-2.86	0.18	-0.81	-1.81	-1.81	-0.19	0.98
$\Delta H^\circ$ (KJ mol <sup>-1</sup> )		91.96			-69.34			61.53			-53.63	
$\Delta S^\circ$ (J mol <sup>-1</sup> K <sup>-1</sup> )		318.69			-206.61			205.69			-169.32	



**Table 5. Distribution coefficient and selectivity coefficient of L-Phe-CD/SiO<sub>2</sub>**

Adsorb material	L-Phe-CD/SiO <sub>2</sub>	
	L-Ala	D-Ala
K <sub>d</sub> (mL g <sup>-1</sup> )	988.69	390.79
K	2.53	

nature of adsorption for both enantiomers from 298 K to 308 K, while the value of  $\Delta H^\circ$  was found to be negative because adsorption is exothermic for both enantiomers from 308 K to 323 K. The possible reason of this phenomenon is that the quaternary reaction produced by the amino of L-Phe and carboxyl of Ala is enantiomer, which means high temperature leads to high adsorption capacities. But the process of producing hydrogen bond is exothermic, which means higher temperatures result in low adsorption capacities. Besides, the value of the entropy of Ala enantiomers from 298 K to 308 K is positive, but the value is negative from 308 K to 323 K, which also confirms the above point. What's more, the value of the entropy of L-Ala is higher than that of D-Ala, which on the other side confirming L-Phe-CD/SiO<sub>2</sub> exhibits higher selectivity for L-Ala than D-Ala.

### 8. Adsorption Selectivity

A mixture solution (racemic solution, optical rotation is zero) of the same amount L-Ala and D-Ala dissolved in water, was chosen as the competitive species with L-Phe-CD/SiO<sub>2</sub> for the adsorption selectivity study at the optimum condition. The distribution coefficient (K<sub>d</sub>) and selectivity coefficient (K) are given in Table 5. The prepared chiral L-Phe-CD/SiO<sub>2</sub> shows a significantly higher adsorption capacity for L-Ala than that for D-Ala. The result also indicates that the L-Phe-CD/SiO<sub>2</sub> has high adsorption selectivity for L-Ala over the D-Ala. The reason for the above facts can be accounted for as follows. It is well known that the fine adsorption ability and high binding selectivity of  $\beta$ -cyclodextrin materials for template come from a great deal of the suited cavities. These cavities both suit to L-Ala and D-Ala molecules in size, shape and spatial arrangement of action sites. However, the  $\beta$ -cyclodextrin materials modified by L-phenylalanine could increase the chiral recognition sites, which increases recognition ability of L-Ala, resulting in that the binding ability of L-Phe-CD/SiO<sub>2</sub> for L-Ala is high. Although D-Ala molecule is able to enter into the cavities, the chiral binding sites are unsuitable for D-Ala, resulting in that the binding ability of L-Phe-CD/SiO<sub>2</sub> for D-Ala is weaker. The above facts clearly reveal that L-Phe-CD/SiO<sub>2</sub> has high recognition selectivity and binding affinity for the L-Ala, and could be applied to chiral separation of the racemic alanine acid solution.

### CONCLUSIONS

A chiral L-Phe-CD/SiO<sub>2</sub> with high selectivity performance was prepared based on  $\beta$ -cyclodextrin, 3-glycidoxypropyltriethoxysilane, activated silica gel and L-phenylalanine. The structure, morphology and thermal property of L-Phe-CD/SiO<sub>2</sub> chiral material were characterized by FT-IR, elemental analysis, FESEM and TG analysis. The experimental data were applied to simulate the kinetic models, and the obtained results indicated that the adsorption of Ala on chiral

L-Phe-CD/SiO<sub>2</sub> could be explained by the mechanism of pseudo-second-order. For the prepared L-Phe-CD/SiO<sub>2</sub>, Langmuir and Freundlich isotherm models were fitted well. Moreover, the selectivity experimental results show that the L-Phe-CD/SiO<sub>2</sub> has excellent selectivity for the L-Ala relative to the competition species. The result shows that the prepared L-Phe-CD/SiO<sub>2</sub> could be applied to chiral separation of the racemic alanine acid solution.

### ACKNOWLEDGEMENT

This project was supported by the Agricultural Independent Innovation of Jiangsu Province (CX(11)2032).

### REFERENCES

1. S. Ghosh, A. Z. M. Badruddoza, M. S. Uddin and K. Hidajat, *J. Colloid Interface Sci.*, **354**, 483 (2011).
2. K. Horiike, T. Ishida, H. Tanaka and R. Arai, *J. Mol. Catal. B-Enzym.*, **12**, 37 (2001).
3. X. L. Liu and L. L. Meng, *Korean J. Chem. Eng.*, **30**, 918 (2013).
4. J. A. Shin, Y. G. Lim and K. H. Lee, *J. Org. Chem.*, **77**, 4117 (2012).
5. O. Stephany, S. Tisse, G. Coadou, J. P. Bouillon, V. Peulon-Agasse and P. Cardinael, *J. Chromatogr. A*, **1270**, 254 (2012).
6. Y. Q. Feng, M. J. Xie and S. L. Da, *Anal. Chim. Acta*, **403**, 187 (2000).
7. N. Shah, J. H. Ha, M. Ul-Islam and J. K. Park, *Korean J. Chem. Eng.*, **28**, 1936 (2011).
8. J. Vozka, K. Kalikova, L. Janeckova, D. W. Armstrong and E. Tesarova, *Anal. Lett.*, **45**, 2344 (2012).
9. H. Kenjiro, T. Keiko, M. Masahito and W. Hideo, *J. Chromatogr. A*, **355**, 383 (1986).
10. Y. Liu, B. H. Han, B. Li, Y. M. Zhang, P. Zhao, Y. T. Chen, T. Wada and Y. Inoue, *J. Org. Chem.*, **63**, 1444 (1998).
11. Y. Liu, B. H. Han, S. X. Sun, T. Wada and Y. Inoue, *J. Org. Chem.*, **64**, 1487 (1999).
12. S. Y. Wang, Y. Dai, J. H. Wu, J. Zhou, J. Tang and W. H. Tang, *J. Chromatogr. A*, **1277**, 84 (2013).
13. P. Paik, Y. Mastai, I. Kityk, P. Rakus and A. Gedanken, *J. Solid. State. Chem.*, **192**, 127 (2012).
14. P. Paik, A. Gedanken and Y. Mastai, *Micropor. Mesopor. Mater.*, **129**, 82 (2010).
15. P. Paik, A. Gedanken and Y. Mastai, *ACS Appl. Mater. Int.*, **1**, 1834 (2009).
16. P. Paik, A. Gedanken and Y. Mastai, *J. Mater. Chem.*, **20**, 4085 (2010).
17. A. Kaveh, G. A. Behdad and H. A. K. Amirhossein, *J. Inorg. Mater.*, **27**, 660 (2012).
18. S. B. Wang, C. W. Ng, W. T. Wang, Q. Li and L. Q. Li, *J. Chem. Eng. Data*, **57**, 1563 (2012).
19. R. Breslow, M. F. Czarniecki, J. Emert and H. Hamaguchi, *J. Am. Chem. Soc.*, **102**, 762 (1980).
20. J. Pan, X. Zou, X. Wang, W. Guan, Y. Yan and J. Han, *Chem. Eng. J.*, **162**, 910 (2010).
21. J. F. Guo and B. J. Gao, *Acta Polym. Sinica*, **1**, 47 (2012).
22. K. Fujimura, T. Ueda and T. Ando, *Anal. Chem.*, **55**, 446 (1983).
23. G. Crini, N. Morin and M. Morcellet, *J. Chromatogr. Sci.*, **37**, 121 (1999).

24. G. Crini, M. Morcellet and G. Torri, *J. Chromatogr. Sci.*, **34**, 477 (1996).
25. G. Crini and M. Morcellet, *J. Chromatogr. Sci.*, **34**, 485 (1996).
26. G. Crini, Y. Lekchiri and M. Morcellet, *Chromatographia*, **40**, 296 (1995).
27. Y. S. Ho and G. McKay, *Water Res.*, **33**, 578 (1999).
28. Y. S. Ho and G. McKay, *Process Biochem.*, **34**, 451 (1999).
29. M. Mazzotti, *J. Chromatogr. A*, **1126**, 311 (2006).
30. S. J. Allen, G. McKay and J. F. Porter, *J. Colloid Interface Sci.*, **280**, 322 (2004).
31. K. Fytianos, E. Voudrias and E. Kokkalis, *Chemosphere*, **40**, 3 (2000).
32. K. L. Li and X. H. Wang, *Bioresour. Technol.*, **100**, 2810 (2009).